Structural and luminescent properties of europium doped TiO_2 thick films synthesized by the ultrasonic spray pyrolysis technique

2009 J. Phys. D: Appl. Phys. 42 095102

(http://iopscience.iop.org/0022-3727/42/9/095102)

IOP PUBLISHING JOURNAL OF PHYSICS D: APPLIED PHYSICS

J. Phys. D: Appl. Phys. **42** (2009) 095102 (7pp) doi:10.1088/0022-3727/42/9/095102

Structural and luminescent properties of europium doped TiO_2 thick films synthesized by the ultrasonic spray pyrolysis technique

E Zaleta-Alejandre[1], M Zapata-Torres[1], M García-Hipólito[2], M Aguilar-Frutis[1], G Alarcón-Flores[1], J Guzmán-Mendoza[1] and C Falcony[3]

[1] Centro de Investigación en Ciencia Aplicada y Tecnología Avanzada-IPN; Legaria # 694, Col. Irrigación, Del. Miguel Hidalgo, México D.F.
[2] Instituto de Investigaciones en Materiales-Universidad Nacional Autónoma de México; A.P. 70-360, Coyoacán 04510, México D.F.
[3] Centro de Investigación y de Estudios Avanzados-IPN; Departamento de Física, Apdo. Postal 14-470, Del. Gustavo A. Madero, C.P. 07000, México, D.F.

E-mail: ezaletaa@ipn.mx

Received 16 December 2008, in final form 14 February 2009
Published 15 April 2009
Online at stacks.iop.org/JPhysD/42/095102

Abstract
The structural and luminescent properties of trivalent europium-doped titanium dioxide films synthesized by the ultrasonic spray pyrolysis technique at several substrate temperatures are reported. These films are nanocrystalline and present a mixture of tetragonal (anatase and rutile) crystal structures of the titania as determined by x-ray diffraction. The rutile crystal structure became predominant as the substrate temperature during deposition was increased. Under UV and electron beam excitation, these coatings showed strong luminescence due to f–f transitions and the dominant transition was the hypersensitive $^5D_0 \rightarrow {}^7F_2$ red emission of Eu^{3+}. The photo- and cathodoluminescence characteristics of these films were studied as a function of growth parameters such as substrate temperature and europium concentration. Excitation with a wavelength of 396 nm resulted in photoluminescent emission peaks located at 557, 580, 592, 615, 652 and 703 nm, associated with the electronic transitions of the Eu^{3+} ion. The photoluminescence (PL) intensity as a whole is observed to decrease as the deposition temperature is increased. Also, with increasing doping concentration, a quenching of the PL is observed. The chemical composition and surface morphology characteristics of the films are also reported.

1. Introduction

Titanium dioxide (TiO_2) is one of the most extensively studied metal oxides because of its potential applications as photo-catalyzer, self-cleaning material, ultrawhite pigment, light scatterer, bio-compatible material and high refractive material for optoelectronic devices [1–5], and also in waste water purification [6], in solar cells [7], as a gas sensor material [8], host lattice for phosphors [9] and thermoluminescent applications [10], among others. TiO_2 films have been deposited by different methods, such as ablation laser deposition [11], RF-sputtering [12], sol–gel processes [13], chemical vapour deposition (CVD) [14] and ultrasonic spray pyrolysis (USP) [15]. The USP technique is considered as a low cost process, versatile, easily scalable to industrial applications and appropriate for the deposition of metallic oxide films doped with rare earth ions [16, 17].

TiO_2 has also attracted much attention for many years due to its physical properties, which show variations influenced by impurities, oxygen defects and crystalline modifications. In

particular, TiO_2 is a promising host material for sensitizing luminescence of Eu^{3+} ions because of its low cost and high transparency in the visible-light region. Luminescent nanomaterials, on the other hand, have attracted increasing technological and industrial interest. This interest has been centred mainly on their optical properties, which have some influence on the structure of emission spectra, quantum efficiency, concentration quenching, etc. Recently, several research groups [18, 19] have studied the optical spectroscopy of nanostructured metal oxides as hosts for rare earth ions to improve the total luminescence efficiency in advanced phosphor and photonic materials.

The luminescent properties of the rare earth ions incorporated into a variety of metallic oxides, organic and semiconductor materials (crystalline and amorphous) have been studied for many years. Applications such as x-ray imaging, scintillators, optical fibres, flat panel displays, radiation sensors, lasers and solid state devices with white light emission have been reported [20]. One of the most promising ways to produce white light (in solid state devices) is the use of a light emitting diode (LED) that emits UV radiation in the wavelength range from 360 to 400 nm in combination with green and red emitting phosphors. This approach yields a more balanced white spectrum than the traditional blue emitter + yellow phosphor LED, and more simplified control than the combination of individual red, green and blue LEDs to generate white light. Then new efforts are being made in order to develop new phosphors that emit a more intense component in the red region. Semiconducting oxides are promising phosphor materials because of their wide band gap and low absorbance in the visible region. Among these oxides, the red emitting phosphor $TiO_2:Eu^{3+}$ studied in the present investigation shows an excellent possibility for white LED applications, since its main excitation band is centred at 396 nm, which coincides with the current UV light emission of GaN-based LEDs [21].

The results of europium doped TiO_2 thick films growth by the USP technique on glass substrates are reported in this paper. The above-mentioned deposition technique is a simple, low cost and highly effective process to synthesize the rare earth ion Eu^{3+} doped TiO_2. The deposited films show strong photoluminescence (PL) and cathodoluminescence (CL) emission intensities, as a function of the deposition parameters. In addition, the crystalline structure and surface morphology characteristics of these films are presented.

2. Experimental details

The USP technique was used to deposit europium-doped titanium oxide films. In this technique, a mist of a solution containing the precursor materials to be deposited is ultrasonically generated and sprayed through a nozzle over a substrate previously heated. The solvents in the spraying solution are vaporized when the mist of the solution gets to the hot substrate, producing a pyrolytic reaction resulting in a solid oxide coating on the substrate. The nozzle is located approximately 1 cm above the substrate. The starting solution was prepared dissolving metallic titanium in peroxide (H_2O_2) at 0.025 M concentration. Typically, 0.1 g of titanium were mixed with 100 ml of H_2O_2 plus 1 mL of ammonium hydroxide. This mixture was stirred during 150 min, at room temperature, until complete dissolution of the titanium was reached. Doping with europium was achieved by adding $EuCl_3 \cdot 6H_2O$ (99.9%) to the spraying solution in the range from 0 to 16 atomic percent (at%). The carrier gas was dry purified air at a pressure of 40 psi, at a flow rate of 10 L min^{-1}. The solution flow rate was 3 mL min^{-1}. The substrate temperature (T_s) during deposition was in the range from 300 to 500 °C in steps of 50 °C; the substrates used were Corning 7059 glass slides. The deposition time was adjusted (10 to 12 min) to deposit films with approximately the same thickness. The thickness of the films studied was about 10 μm, as measured by a Sloan Dektak IIA profilometer. The crystalline structure of the deposited films was analysed by x-ray diffraction, using a Siemens D-5000 diffractometer with wavelength radiation of 1.5406 Å (Cu K_α). The measurements were performed in glancing angle geometry at 1.5°. The chemical composition of the films was measured using energy dispersive spectroscopy (EDS) with a Cambridge–Leica electron microscope mod. Stereoscan 440 equipped with a beryllium window x-ray detector. SEM micrographs, on the surface morphology of the films, were obtained by means of the above-mentioned microscope. CL measurements were performed in a stainless steel vacuum chamber with a cold cathode electron gun (Luminoscope, model ELM-2 MCA, RELION Co.). Samples were placed inside the vacuum chamber and evacuated up to 10^{-2} Torr. The electron beam was deflected through a 90° angle to bombard the luminescent material normal to the surface. The emitted light from the samples was collected with an optical fibre bundle leading to a spectrofluorometer SPEX Fluoro-Max-P. All spectra were obtained at room temperature. The accelerating voltage in the CL measurements was in the range from 4 to 20 kV with a current of 0.5 mA. The spot size of the beam on the surface sample was approximately 3 mm in diameter. In addition, the PL measurements (excitation and emission spectra) were carried out using the above-mentioned spectrofluorometer.

3. Results and discussion

Figure 1 shows the XRD diffractograms for $TiO_2:Eu^{3+}$ (10 at% in the starting solution) at five different substrate temperatures, 300, 350, 400, 450 and 500 °C. In all these cases, it is possible to observe a combination of the anatase and rutile tetragonal phases of TiO_2. The strongest reflections are centred at 25.28° (anatase, JCPDS-211272) and 27.44° (rutile, JCPDS-211276) which correspond to lines (1 0 1) and (1 1 0), respectively, indicating a preferential orientation of the crystallites. Interestingly, the width of those peaks remains constant to any substrate temperature.

The crystallite sizes, calculated from the line-shape analysis using the Scherrer formula ($t = 0.9\lambda/B\cos\theta_B$) [22] of the above-mentioned peaks, were 15 nm and 10 nm, respectively. Table 1 summarizes the relative chemical content of the oxygen, titanium and europium present in the films deposited at 300 °C as a function of the content of the

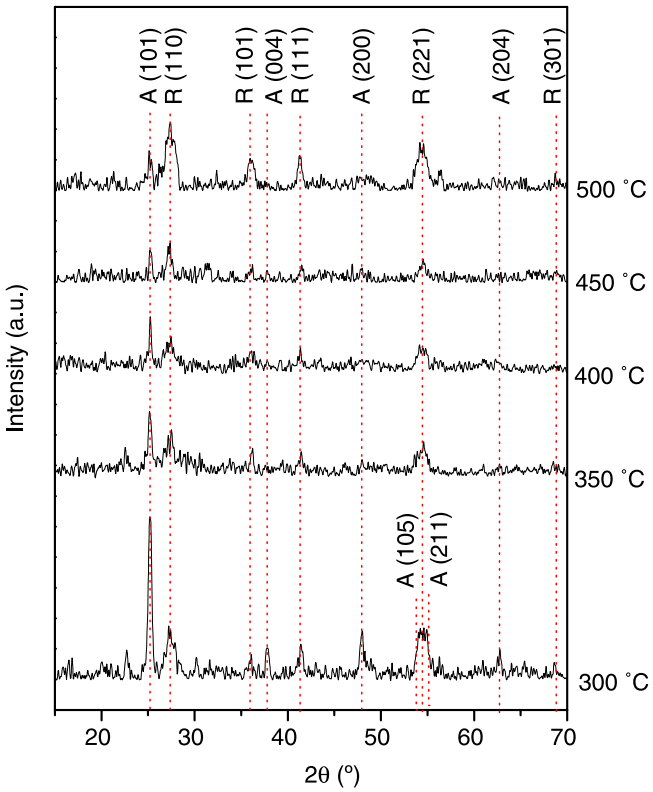

Figure 1. XRD patterns for europium-doped titanium dioxide films deposited at 300, 350, 400, 450 and 500 °C.

(This figure is in colour only in the electronic version)

Table 1. Atomic percent content of the oxygen, titanium and europium in the films as measured by EDS for different $EuCl_3$ concentrations in the spraying solution. In this case the substrate temperature was 300 °C.

$EuCl_3$ concentration in the spraying solution (at%)	Oxygen	Titanium	Europium
0	60.9	39.1	0.0
4	60.5	39.0	0.5
8	60.1	38.7	1.2
10	60.2	38.1	1.7
12	60.5	37.6	1.9
16	60.1	37.1	2.8

europium chloride incorporated in the spraying solution. A slight reduction in the relative content of titanium and an increase in the relative content of europium are observed, as expected, when the doping concentration is increased. The oxygen content remains approximately constant. Table 2 shows similar results to those in table 1 but as a function of the deposition temperature, keeping constant the doping concentration ($EuCl_3$, 10 at%) in the starting solution. The relative content of oxygen rises and a reduction in the relative content of titanium and europium are observed as the substrate temperature increases. At low substrate temperatures the surface thermal energy is probably insufficient for a complete dissociation of the reacting molecules and to evaporate the solvents. As the deposition temperature increases, a larger thermal energy is available to reach a complete decomposition and processing of the material arriving at the substrate. This

Table 2. Atomic percent content of the oxygen, titanium and europium inside the films as determined by EDS for different substrate temperatures. In this case, the $EuCl_3$ concentration in the spraying solution was 10 at%.

Substrate temperature (°C)	Oxygen	Titanium	Europium
300	60.2	38.1	1.7
350	62.5	36.3	1.2
400	63.1	35.9	1.0
450	64.0	35.2	0.8
500	64.8	34.5	0.7

condition promotes the evaporation of the residual products and the formation of the crystallites of titanium dioxide which make the incorporation of europium diminish. With the crystallization of TiO_2 the relative contents of oxygen and titanium approach their ideal values: O (66 at%), Ti (33 at%). The observed deviations of these values are due to the incorporation of the activator ions, Eu^{3+}.

SEM micrographs of the surface morphology of the $TiO_2:Eu^{3+}$ (10 at%) coatings deposited at 300, 400, 500 °C and a cross section of that deposited at 300 °C are shown in figure 2. The films are rough and continuous with good adherence to the substrate. It is observed that the surface morphology of the films depends lightly on the deposition temperature. Films deposited at 300 °C present rough and porous surfaces with hollow spherical particles; presumably in this case the substrate thermal energy is not enough to process the material completely to form closed and compact surfaces. Coatings deposited at 400 and 500 °C show slightly more compact surfaces than those deposited at 300 °C. As the deposition temperature is increased, a rough surface with a more open network is observed; in this case most of the spherical particles are cracked producing films with higher surface area. These characteristics are probably obtained because at higher substrate temperatures the deposited precursors have larger surface kinetic energy, which produces a more complete pyrolytic reaction of the reactant materials. In addition, the cross section of the sample deposited at 300 °C exhibits a nodular growth of the film rather than a columnar one. It is possible to observe that the coating is formed by two sections: one constituted by a 'solid' layer of approximately 2–3 μm in thickness and above the previous one, the other composed of a 'more porous' section of dispersed hollow spherical particles of diverse sizes (typically 1–2 μm). In addition, the thickness observed is similar to the value measured by the profilometer.

Figure 3 shows the PL excitation spectrum of $TiO_2:Eu^{3+}$ (10 at% in the spraying solution) films synthesized at 300 °C for 10 min. This spectrum was taken for the 615 nm emission wavelength at which the maximum emission intensity peak is observed. The excitation spectrum is the true fingerprint of the characteristic absorption lines corresponding to the $4F^n \rightarrow 4F^n$ transitions of europium ions. In this case, six bands can be observed centred at 334 nm, 363 nm, 383 nm, 396 nm, 416 nm and 466 nm, and the last five bands correspond to the absorption electronic transitions $^7F_{0.1} \rightarrow {}^5D_4$, $^7F_{0.1} \rightarrow {}^5L_7$, $^7F_{0.1} \rightarrow {}^5L_6$, $^7F_{0.1} \rightarrow {}^5D_3$, $^7F_{0.1} \rightarrow {}^5D_2$ of the Eu^{3+} ion, respectively. The strongest peak emission occurs at 396 nm.

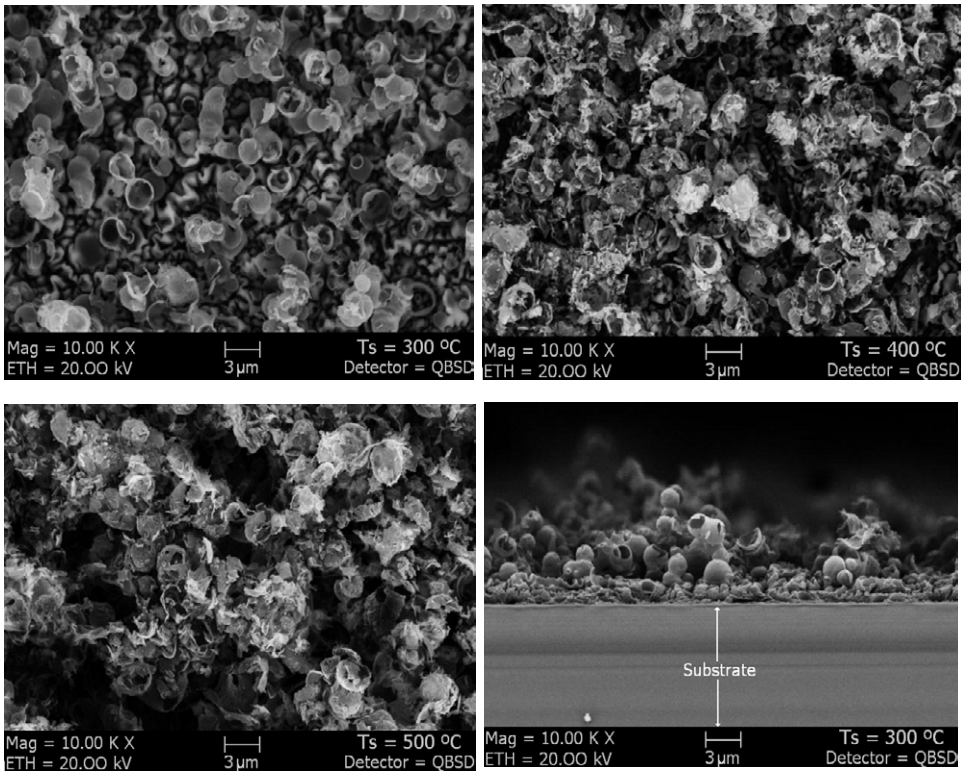

Figure 2. SEM micrographs of surface morphology of TiO_2: Eu (10 at%) films. The deposition temperatures were 300, 400 and 500 °C. In addition, a cross section of the sample deposited at 300 °C is shown.

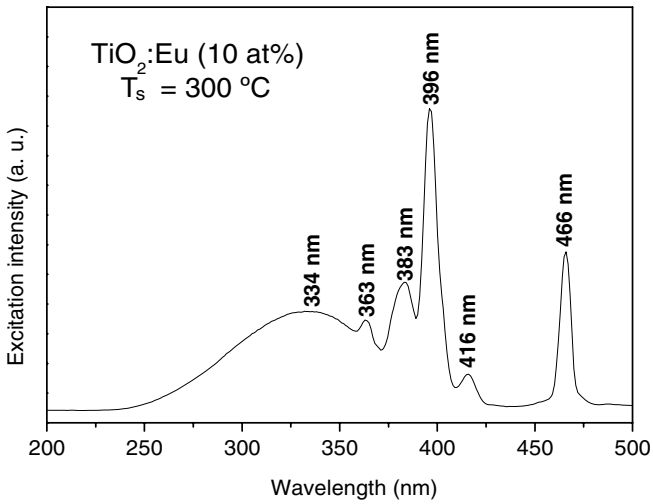

Figure 3. Excitation spectrum for a TiO_2: Eu (10 at%) film. The substrate temperature was 300 °C and the emission was fixed at 615 nm.

The wide band centred at 334 nm could be associated with host lattice absorption and indicates the presence of titanium species such as tetrahedral titanium (IV). This absorption band is generally associated with the electronic excitation of the valence band O 2p electron to the conduction band titanium 3d level [23]. A mechanism for the energy transfer process is presented in [24]; when the UV radiation is absorbed in the band of the TiO_2 host lattice the energy is relaxed to the defect states; since the defect energy position of the TiO_2 host is higher than that of the emitting state $^5D_0$ of Eu^{3+} ions, energy transfer to the crystal field states of Eu^{3+} ions takes place, resulting in an efficient PL.

The PL emission spectra of the $TiO_2 : Eu^{3+}$ nanocrystalline films are shown in figure 4. In this case, the substrate temperature was 300 °C and the excitation wavelength was 396 nm. These coatings exhibit a strong red emission under the ultraviolet irradiation. The $^5D_0$ emission of Eu^{3+} ions has six characteristic peaks centred at 557 nm, 580 nm, 592 nm, 615 nm, 652 nm and 703 nm, which are assigned to the $^5D_1 \rightarrow {}^7F_2$, $^5D_0 \rightarrow {}^7F_0$, $^5D_0 \rightarrow {}^7F_1$, $^5D_0 \rightarrow {}^7F_2$, $^5D_0 \rightarrow {}^7F_3$ and $^5D_0 \rightarrow {}^7F_4$ transitions, respectively. From this figure, it can be seen that the $^5D_0$ emission of Eu^{3+} is intensified with the increase in Eu^{3+} content, and the emission intensity is the strongest at about 10 at% of $EuCl_3$ concentration in the starting solution (1.7 at% as measured by EDS). At higher Eu^{3+} concentrations, the emission intensity is notably decreased. This is the well-known concentration quenching effect, which can be explained by the cross-relaxation mechanisms [25]. At a Eu^{3+} concentration of 1.7 at%, the Eu–O–Ti bonds may be saturated and at higher concentrations the spatial separation between Eu^{3+} ions becomes smaller and, therefore, the cross-relaxation rate is higher.

The behaviour of PL emission intensity of $TiO_2 : Eu^{3+}$ (1.7 at%) coatings, as a function of the substrate temperature, is shown in figure 5. The PL emissions decrease with increasing deposition temperature. The maximum PL emission intensity is observed for samples deposited at 300 °C. The excitation wavelength was 396 nm. As the substrate temperature rises, an improved crystallization of the host material is obtained,

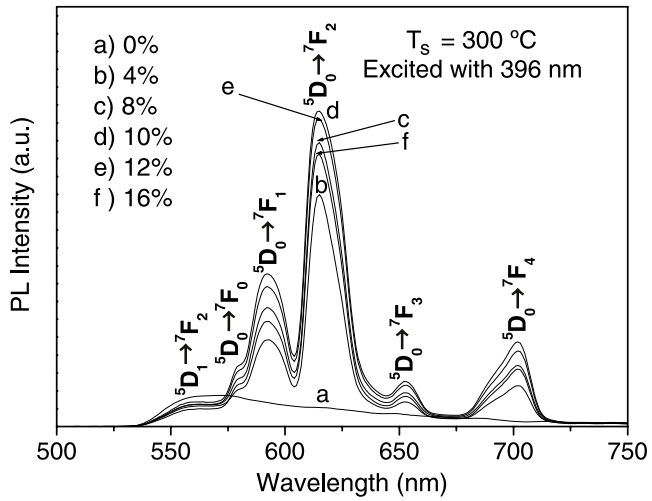

Figure 4. Behaviour of PL emission intensity as a function of the doping concentration for TiO_2: Eu films synthesized at $T_s = 300\,^{\circ}C$ and excited by 396 nm radiation.

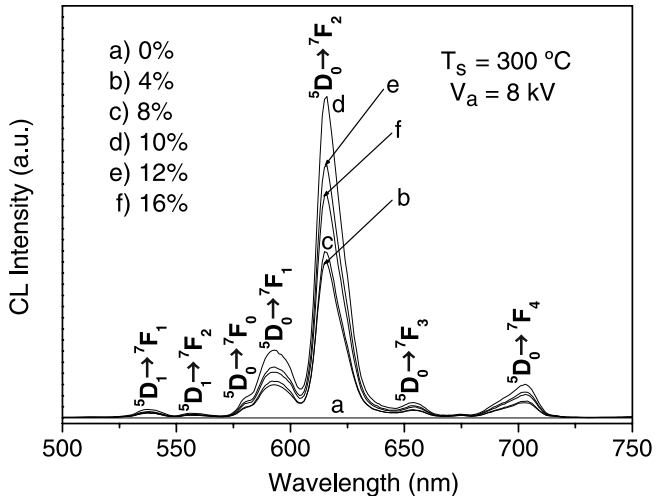

Figure 6. CL emission spectra for TiO_2: Eu films changing the doping concentration, under 8 kV electron accelerating voltage. $T_s = 300\,^{\circ}C$.

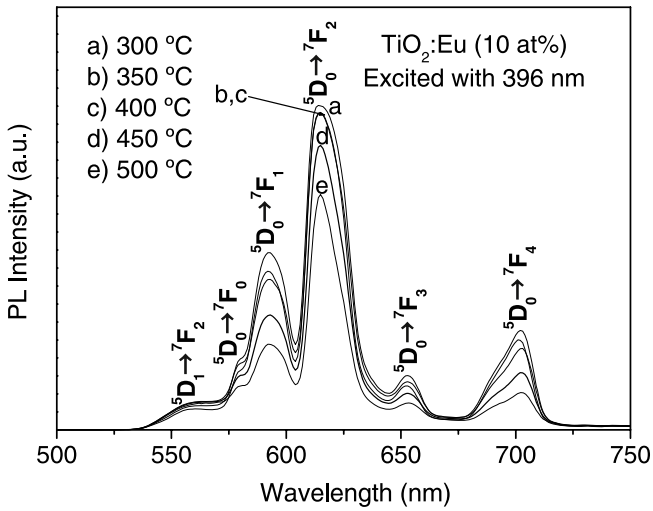

Figure 5. Behaviour of PL emission intensity as a function of the substrate temperature for TiO_2: Eu (10 at%) films, excited by 396 nm radiation.

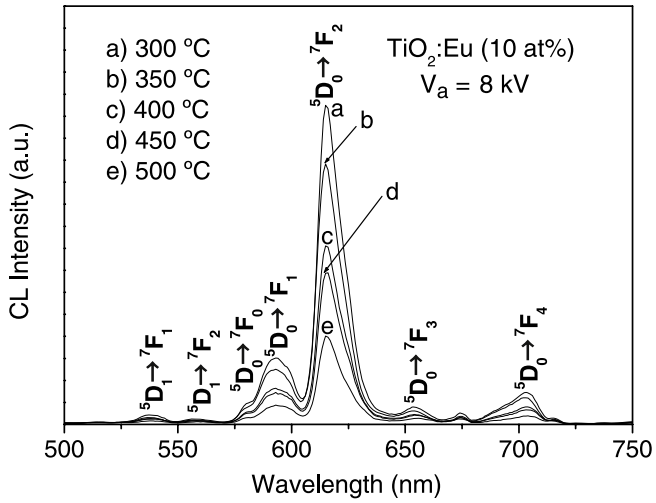

Figure 7. Behaviour of CL emission intensity as a function of the substrate temperature for TiO_2: Eu (10 at%) films, the electron accelerating voltage was 8 kV.

as shown by the XRD measurements. In this case, the nanocrystalline titanium dioxide tetragonal anatase phase transforms into the tetragonal rutile phase which presents a higher density, making it more difficult for Eu^{3+} ions to substitute Ti^{4+} due to their different chemical properties and ionic radii. The ionic radii of Eu^{3+} (0.95 Å) are larger than that of Ti^{4+} (0.68 Å), so Eu^{3+} can hardly enter into the TiO_2 lattice. The reduction in the PL intensity as the substrate temperature rises may be due to the fact that the amorphous titania and/or the nanocrystalline anatase phase are partially transformed into rutile phase in the process. As a result, the Eu^{3+} ions, which were dispersed uniformly in the original material, tend to be segregated so Eu^{3+} ions are inclined to relocate into the boundary of the TiO_2 nanocrystals. This might cause Eu–Eu interaction or the formation of Eu_2O_3 nanoaggregates which could act as quenchers for the photoluminescent emission intensity.

The CL spectra as a function of activator concentration in the spraying solution are shown in figure 6, under 8 kV electron accelerating potential (in these cases $T_s = 300\,^{\circ}C$). The characteristics of these spectra are similar to those for PL, except for the appearance of the trivalent europium $^5D_1 \rightarrow {}^7F_1$ transition. Once again a concentration quenching is observed for doping concentration higher than 10 at% of $EuCl_3$ in the starting solution.

Figure 7 shows the CL emission intensity behaviour, as a function of the deposition temperature. In this case, the doping concentration was 10 at% and the electron accelerating voltage was 8 kV. The maximum emission intensity is obtained for samples deposited at 300 °C. These results are similar to those obtained in the PL measurements. Once again, the $^5D_1 \rightarrow {}^7F_1$ transition of the trivalent Eu^{3+} ion appears in these spectra.

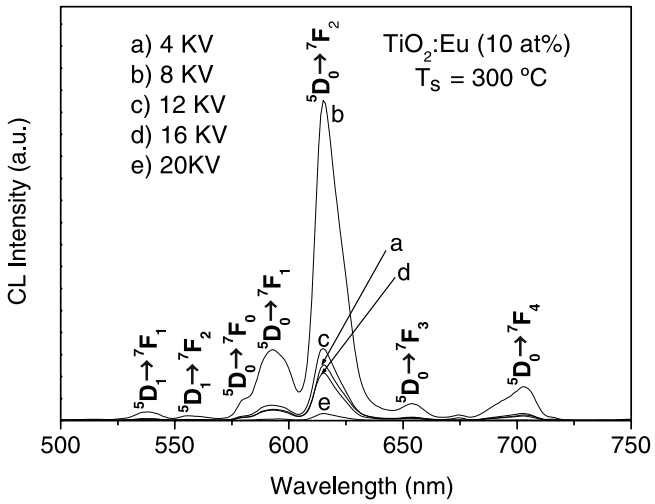

Figure 8. Behaviour of CL emission intensity as a function of the electron accelerating voltage for TiO_2: Eu (10 at%) films. The substrate temperature was 300 °C.

Figure 8 shows plots of CL spectra measured under steady-state excitation with accelerating beam voltages from 4 to 20 kV. The deposition substrate temperature was 300 °C and the doping concentration, in the start solution, was 10 at% for this sample. The observed emission spectra consist of seven bands characteristic of the Eu^{3+} ion. In this case, the best emission intensity is produced by an electron accelerating voltage of 8 kV. Using higher voltages, a CL quenching is observed. When high voltages are used the samples trap electrical charge which interferes with the incident electron beam. Also, impurities adsorbed at the surface of luminescent materials or surface defects often become quenchers and may, by quenching the emission near the surface, produce a 'dead-voltage layer'. The existence of the dead voltage is often ascribed to the nonradiative surface recombination of the carriers (electron–hole pairs). Other possible effects relative to quenching of CL emissions are (a) saturation of luminescent centres, whereby the majority of the centres are already in excited states, leaving an insufficient quantity of available centres in the ground state free to accept energy from the excited carriers [26, 27], (b) thermal quenching, due to the local heating, by energetic electrons, of the luminescent material and (c) the Auger effect which produces ejection of electrons leaving the luminescent centres de-excited [28]. The exact nature of the CL emissions quenching, for this case, is still unknown and needs additional investigation.

4. Conclusions

Strong red PL and CL emissions from $TiO_2:Eu^{3+}$ films, synthesized by the USP technique, have been observed. The $TiO_2:Eu^{3+}$ films prepared by this technique possess many desirable properties such as high homogeneity and high surface area at low cost and low deposition temperatures. The XRD patterns showed that for all substrate temperatures we had a mixture of the anatase and rutile phases of TiO_2. Using the Scherrer formula, the crystallite sizes of the synthesized films were estimated to be around 15 nm. The excitation spectrum showed that radiation of 396 nm is the optimal to excite the red band emission centred at 615 nm. Europium doped-TiO_2 films exhibited high pure red characteristic light emission from the Eu^{3+} ion upon excitation of the TiO_2 host lattice (334 nm) due to energy transfer from the TiO_2 to the excited state energy levels of this ion; in addition, the excitation band peaked at 396 nm indicates that there is also a direct excitation of the Eu^{3+} ions. A PL and CL concentration quenching with increasing activator concentration was observed above the optimum doping concentration (1.7 at%, as measured by EDS). In addition, a luminescence (PL and CL) quenching was observed with increasing substrate temperature. An electron accelerating potential of 8 kV produced the best CL emission intensity. Since PL emission spectra (excited by a wavelength of 396 nm) showed similar europium transitions as compared with CL emission spectra, this material could be a good candidate for use in both applications involving photon or electron beam excitations. Finally, it should be stressed that there are no reports in the literature, to the best of our knowledge, about the CL and PL characteristics of nanostructured red emitting $TiO_2:Eu^{3+}$ films deposited by the USP technique.

Acknowledgments

The authors thank Leticia Baños (XRD measurements), Omar Novelo and Miguel Angel Aguilar Mendez (SEM-EDS measurements), M Guerrero and Z Rivera for the technical support provided. They also thank the National Council for Science and Technology in México (CONACyT) and SIP-IPN for the financial support through the programme No 966.

References

[1] Carp O, Huisman C L and Reller A 2004 *Prog. Solid State Chem.* **32** 33
[2] Hayakawa S, Liu Y, Okamoto K, Tsuru K and Osaka A 2005 *Mater. Res. Soc. Symp. Proc.* **845** AA6.9.1
[3] Fujita K, Konishi J, Nakanishi K and Hirao K 2004 *Appl. Phys. Lett.* **85** 5595
[4] López T, Ortiz-Islas E, Manjarrez J, Reinoso F R, Sepúlveda A and González R D 2006 *Opt. Mater.* **29** 70
[5] Peng X S, Wang J P, Thomas D F and Chen A C 2005 *Nanotechnology* **16** 2389
[6] Ahmed M and Attia Y A 1995 *J. Non-Cryst. Solids* **186** 402
[7] Barbé C J, Arendse F, Comte P, Jirousek M, Lenzmann F, Shklover V and Gratzel M 1997 *J. Am. Ceram. Soc.* **80** 3157
[8] Ferroni M, Guidi V, Martinelli G, Faglia G, Nelli P and Sberveglieri G 1996 *Nano Strct. Mater.* **7** 709
[9] Zeng Q G, Ding Z J and Zhang Z M 2006 *J. Lumin.* **118** 301–7
[10] Azorín-Vega J C, Azorín-Nieto J, García-Hipólito M and Rivera-Montalvo T 2007 *Radiat. Meas.* **42** 613–6
[11] Zhu M, Chikyow T, Ahmet P, Naruke T, Murakami M, Matsumoto Y and Koinuma H 2003 *Thin Solid Films* **441** 140–4
[12] Gao P, Meng L J, dos Santos M P, Teixeira V and Andritschky M 2000 *Thin Solid Films* **32** 377–8
[13] Conde-Gallardo A, García-Rocha M, Palomino-Merino R, Velásquez-Quesada M P and Hernández-Calderón I 2003 *Appl. Surf. Sci.* **212–213** 583–8

[14] Asahi R and Taga Y 2001 *Phys. Rev.* B **61** 7459
[15] Weng Wenjian, Ma Ming, Du Piyi, Zhao Gaoling, Shen Ge, Wang Jianxun and Han Gaorong 2005 *Surf. Coat. Technol.* **198** 340–4
[16] García-Hipólito M, Caldiño U, Alvarez-Fregoso O, Alvarez-Pérez M A, Martínez-Martínez R and Falcony C 2007 *Phys. Status Solidi* a **204** 2355–61
[17] Ramos-Brito F, García-Hipólito M, Alejo-Armenta C, Alvarez-Fragoso O and Falcony C 2007 *Phys. D: Appl. Phys.* **40** 6718–24
[18] Hasse M, Riwotski K, Meyssana H and Kornowski A 2000 *J. Alloys Compounds* **191** 303–4
[19] Tissue B M 1998 *Chem. Mater.* **10** 2837
[20] Blasse G and Grabmaier B C 1994 *Luminescent Materials* (Berlin: Springer)
[21] Rodríguez-García C E, Perea-López N, Hirata G A and DenBaars S P 2008 *J. Phys. D: Appl. Phys.* **41** 092005 4pp
[22] Cullity B D and Stock S R 2001 *Elements of X-Ray Diffraction* (Englewood Cliffs, NJ: Prentice Hall) 3rd edn pp 167–71
[23] Sreethawong T, Suzuki Y and Yoshikawa S 2005 *Int. J. Hydrog. Energy* **30** 1053
[24] Frindell K L, Bartl M H, Robinson M R, Bazan G C, Popitsch A and Stuckya G D 2003 *J. Solid State Chem.* **172** 81–8
[25] Schmechel R, Kenndy M, Seggern H V, Winkler H, Kolbe M, Fischer R A, Li X, Benker A, Winterer M and Hahn H 2001 *J. Appl. Phys.* **89** 1679
[26] Hase T, Kano T, Nakasawa E and Yamamoto H 1990 Phosphors materials for cathode-ray tubes *Advances in Electronics and Electron Physics* vol 79 (New York: Academic) p 271
[27] de Leeuw D M and tHoof G W 1983 *J. Lumin.* **28** 275
[28] Imanaga S, Yocono S and Hosima T 1980 *Japan. J. Appl. Phys.* **19** 41